Supplementary Information for

Dynamic terahertz wavefront control using stretchable single-walled carbon nanotube-based metasurfaces

Jingwen He[1], Guibin Li[2], Arina V. Radivon[3,4], Liang Qin[1], Linjie Shao[5], Sijia Wang[1], Tong Nan[6], Kirill I. Zaytsev[4], Nikita I. Raginov[7], Maria G. Burdanova[3,4], Albert G. Nasibulin[7], Dmitry V. Krasnikov[7], Yan Zhang[2,*]

[1] *National Physical Experiment Teaching Demonstration Center, Department of Physics, School of Physical Science and Engineering, Beijing Jiaotong University, Beijing, 100044, China*
[2] *Beijing Key Laboratory of Terahertz Optoelectronics, Ministry of Education, Beijing Advanced Innovation Center for Imaging Theory and Technology, Department of Physics, Capital Normal University, Beijing 100048, China*
[3] *Moscow Center for Advanced Studies, Kulakova str. 20, Moscow, 123592, Russia*
[4] *Prokhorov General Physics Institute of the Russian Academy of Sciences, Moscow, 119991, Russia*
[5] *The Dodd-Walls Centre for Photonic and Quantum Technologies, Department of Physics, University of Otago, Dunedin 9016, New Zealand*
[6] *School of Physics, Harbin Institute of Technology, Harbin 150001, China*
[7] *Skolkovo Institute of Science and Technology, Moscow, 121205, Russia*

[*] *Corresponding author: yzhang@cnu.edu.cn*

Note 1. Study on the characteristics of metasurface phase-tuning unit based on single-walled carbon nanotubes (SWCNTs)

Fig. S1a shows a schematic illustration of the stretchable metasurface based on SWCNTs, with the inset depicting a single phase-tuning unit in which a grey SWCNT rod is attached to a silicone substrate. In its unstretched state, each unit cell has a period of P = 350 μm, and the SWCNT rod possesses a length of L = 300 μm, a width of w = 80 μm, and an orientation angle of θ. When the unit cell is stretched, its period increases to AP, while the rod width and length scale to Aw and AL, respectively, where A denotes the stretch factor. The electromagnetic response of the unit, including the amplitude and phase of the scattered wave, are evaluated by full-wave simulations in CST Microwave Studio. In the simulation, the metasurface unit cell is illuminated normally from the substrate side by a 0.35 THz LCP wave, with periodic boundary conditions applied. The silicone substrate has a refractive index of 2.62, and the SWCNT film is assigned a conductivity of 6×10^4 S/m. The thicknesses of the SWCNT film and the substrate are 200 nm and 200 μm, respectively. Through optimisation, eight unit-cells with orientation angles of 0°, 19°, 37°, 60°, 90°, 109°, 127°, and 150° are selected as the basic building blocks of the metasurface. The amplitude and phase of the transmitted RCP component of these units under different stretch factor are summarized in Figs. S1b and S1c, respectively. It can be observed that the transmitted intensity remains nearly equal for all units, while the phase exhibits a linear progression, increasing by π/4 with each unit, and covering the full 0 to 2π range. Moreover, under increasing tensile strain, both the amplitude and phase of the scattered RCP wave exhibit negligible variation, confirming the stability of the unit's electromagnetic response upon stretching.

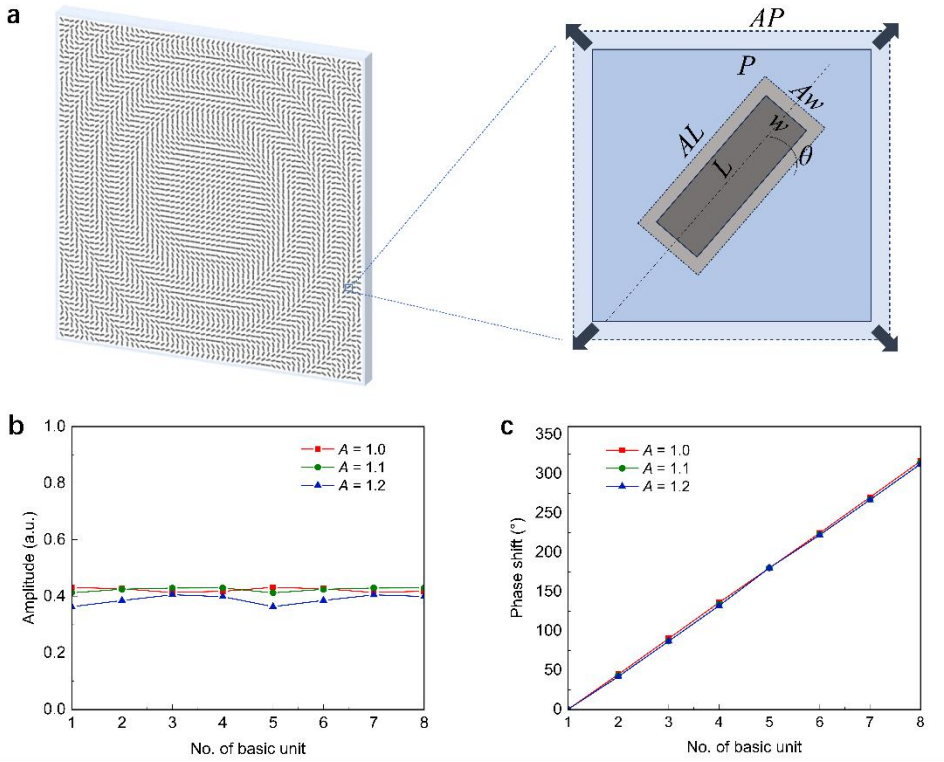

Fig. S1 Schematic and electromagnetic response of the stretchable SWCNT-based metasurface. a Schematic of the metasurface architecture with an inset illustrating the unit cell geometry before and after stretching at a factor of A. **b, c** Amplitude and phase modulation, respectively, of the scattered RCP wave at 0.35 THz by the eight basic unit cells under varying stretch factors (A = 1.0, 1.1, 1.2).

Note 2. Theoretical mechanism of tuneable focusing and beam steering in metasurface lens

When the designed metasurface device is subjected to mechanical stretching, a geometric coordinate transformation $(x, y) \rightarrow (Ax, Ay)$ is induced, where A denotes the stretch factor. This transformation effectively reshapes the overall spatial phase profile. For an ideal lens with a focal point at (x_0, y_0) and a focal length f, the phase distribution in Cartesian coordinates is given by:

$$\varphi(x,y) = \frac{2\pi}{\lambda}(f - \sqrt{(x-x_0)^2 + (y-y_0)^2 + f^2} \quad \text{(S1)}$$

Under the Fresnel approximation ($x, y, x_0, y_0 \ll f$):

$$\sqrt{(x-x_0)^2 + (y-y_0)^2 + f^2} \approx f + \frac{(x-x_0)^2+(y-y_0)^2}{2f} \quad \text{(S2)}$$

yielding

$$\varphi(x,y) \approx -\frac{\pi}{\lambda f}[(x-x_0)^2+(y-y_0)^2] \quad \text{(S3)}$$

Upon uniform stretching by a factor A, the phase distribution transforms as

$$\varphi'(x',y') = \varphi(x,y) = \varphi(x'/A, y'/A) \quad \text{(S4)}$$

Substituting the scaled coordinates, we obtain:

$$\varphi'(x',y') \approx -\frac{\pi}{\lambda f}[(\frac{x'}{A}-x_0)^2+(\frac{y'}{A}-y_0)^2] = -\frac{\pi}{\lambda(A^2 f)}[(x'-Ax_0)^2+(y'-Ay_0)^2] \quad \text{(S5)}$$

Comparing Eq. (S5) with the standard lens phase profile, the new focal position (x_0', y_0') and focal length f' are determined as:

$$f' = A^2 f,\ x_0' = Ax_0,\ y_0' = Ay_0.$$

Consequently, for an off-axis lens with an initial deflection angle θ (where $\tan\theta = x_0/f$), the new deflection angle θ' satisfies:

$$tan\theta' = \frac{x_0'}{f'} = \frac{Ax_0}{A^2 f} = \frac{1}{A}tan\theta \quad \text{(S6)}$$

Note 3. Simulation of the wavefront modulation characteristics of the SWCNT-based metasurface lens under different stretching states

We take the metasurface lens plane as the reference plane z = 0 mm, which serves as the initial propagation plane. The optical field immediately after modulation by the metasurface lens is expressed as $U_0(x_0, y_0, 0) = e^{i\varphi(x_0,y_0)}$, where $\varphi(x_0, y_0)$ denotes the quantized lens phase profile, as illustrated in Fig. 2a. Using $U_0(x_0, y_0,0)$ as the initial field, the complex field at an arbitrary plane along the propagation direction (z > 0) can be computed via the Huygens–Fresnel diffraction integral[1],

$$U(x,y,z) = \frac{z}{j\lambda}\iint U_0(x_0,y_0,0)\frac{\exp(jkr)}{r^2}dx_0dy_0 \quad \text{(S7)}$$

where

$$r = \sqrt{(x-x_0)^2+(x-y_0)^2+z^2}$$

λ is the wavelength in free space, and k=2π/λ is the corresponding free-space wavenumber.

To accurately simulate the optical field modulation characteristics of the metasurface and enable a meaningful comparison with experimental measurements, the finite diameter of the incident THz beam, the effective detection area of the ZnTe crystal, and the position of the detection center must be taken into account. In the experiment, the diameter of the THz beam incident on the metasurface is 20 mm, and the effective area of the detection crystal is a circular region with a diameter of 15.4 mm. The detection crystal is positioned directly behind the sample at a distance z = 11.5 mm. From the simulation, the field distribution on the plane z

= 11.5 mm is obtained as $U_1(x, y)$. The actual field detected by the crystal, denoted $U_1^{'}(x, y)$, is then given by

$$U_1^{'} = U_1 W,$$

where W is a circular window function defined as

$$W(x,y) = \begin{cases} 1, & \sqrt{(x-x_c)^2 + (y-y_c)^2} < R \\ 0, & \sqrt{(x-x_c)^2 + (y-y_c)^2} \geq R \end{cases} \quad \text{(S8)}$$

with R = 7.7 mm (half the crystal diameter), and (x_c, y_c) representing the center of the detection area.

The simulated phase and amplitude distributions of the field $U_1^{'}$ at z = 11.5 mm for different stretch factors are shown in Figs. S2a and S2b, respectively. Propagating $U_1^{'}$ further along the z direction and extracting the field along the line y = 0 mm on successive transverse xy planes yields the spatial distribution of the THz wave in the propagation (xz) plane, as shown in Fig. S2c. It clearly shows that the focal length increases as the sample is stretched. For stretch factors of A = 1.0, 1.1, and 1.2, the focal points are located at 19.5 mm, 23.9 mm, and 27.7 mm, respectively. Under stretch factors of 1.1 and 1.2, the focal spot undergoes backward displacements of 4.4 mm and 8.2 mm, respectively, compared with the unstretched state.

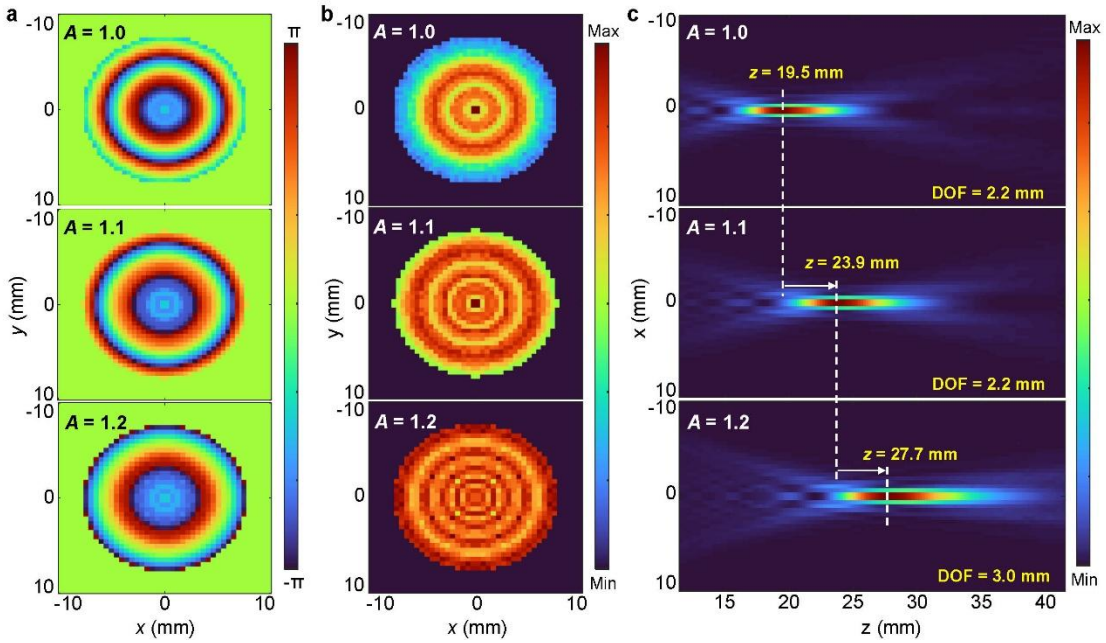

Fig. S2. Simulated optical field distribution of the 0.35 THz RCP component after modulated by the metasurface lens. a Phase and **b** amplitude at the plane of the detection crystal (z = 11.5 mm). (c) Intensity distribution in the propagation plane (xz plane).

Note 4. Simulation of the beam steering characteristics of the SWCNT-based off-axis metasurface lens under mechanical stretching

In the experimental characterization of the off-axis metasurface lens, the detection crystal is positioned in the plane located at z = 13.0 mm directly behind the sample, with its center aligned at (−3.8 mm, 0). Using the phase profile shown in Fig. 4a as the initial phase, the optical field at the metasurface plane (z = 0 mm) is constructed and propagated along the z-direction. The field distribution U_2 at z = 13.0 mm is obtained by using Eq. (S7). After accounting for the effective aperture and the actual position of the detection crystal, the effective detected field distribution is given by $U_2^{'} = U_2 W$, where W is the circular window function centered at (−3.8 mm, 0) with a radius of 7.7 mm. The corresponding amplitude and phase distributions of $U_2^{'}$ are presented in Figs. S3a and S3b, respectively.

By further propagating $U_2^{'}$ along the z-direction and extracting the field along the line y=0 mm on successive xy planes, the spatial distribution of the THz wave in the propagation (xz) plane is reconstructed, as shown in Fig. S3c. The results reveal that under mechanical stretching, the focal spot shifts both axially backward and transversely. For stretch factors A = 1.0, 1.1, and 1.2, the focus are located at (19.6 mm, −20.11°), (24.4 mm, −17.92°), and (28.0 mm, −16.30 °), respectively. Compared with the unstretched state (A = 1.0), the beam undergoes angular deflections of +2.19° and +3.81°, when the sample is stretched to 1.1 and 1.2 times its original length.

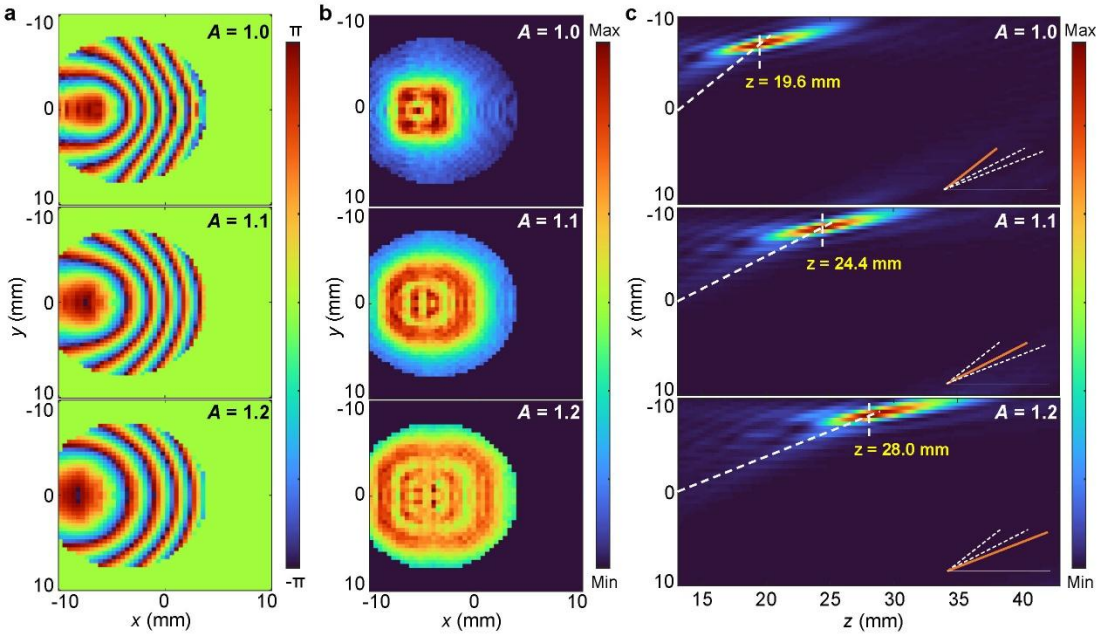

Fig. S3. Simulated optical field distribution of the 0.35 THz RCP component after modulated by the off-axis metasurface lens. a Phase and **b** amplitude at the plane of the

detection crystal (z = 13.0 mm). (c) Intensity distribution in the propagation (xz) plane.

Supplementary Video: Reversible stretching and recovery of the SWCNT-based metasurface sample

The sample was cyclically stretched and released during the experiment, demonstrating excellent mechanical reversibility and stable optical performance with no observable degradation in appearance or functionality.

References

1 Born, M. & Wolf, E. Principles of optics, 561 (Cambridge Univ. Press, 1999).